Available online at www.sciencedirect.com

ScienceDirect

Geochimica et Cosmochimica Acta 259 (2019) 155–169

Geochimica et Cosmochimica Acta

www.elsevier.com/locate/gca

Bacterial GMGTs in East African lake sediments: Their potential as palaeotemperature indicators

Allix J. Baxter [a,*], Ellen C. Hopmans [a], James M. Russell [c], Jaap S. Sinninghe Damsté [a,b,*]

[a] NIOZ Royal Netherlands Institute for Sea Research, Department of Marine Microbiology and Biogeochemistry, and Utrecht University, PO Box 59, 1790 AB Den Burg, Texel, the Netherlands

[b] University of Utrecht, Faculty of Geosciences, PO Box 80.021, 3508 TA Utrecht, the Netherlands

[c] Brown University, Department of Earth, Environmental, and Planetary Sciences, 324 Brook St., Box 1846, Providence, RI 02912, USA

Received 29 August 2018; accepted in revised form 27 May 2019; available online 10 June 2019

Abstract

Glycerol monoalkyl glycerol tetraethers (GMGTs) are a group of membrane spanning lipids produced by some species of archaea and bacteria. They differ from the more commonly studied glycerol dialkyl glycerol tetraethers (GDGTs) in having an additional covalent carbon-carbon bond connecting the two alkyl chain. The relative abundance and distribution of bacterial branched GMGTs (brGMGTs) in surface sediments from a set of East African lakes were studied. The abundance of brGMGTs relative to the brGDGTs is positively correlated to measured mean annual air temperature (MAAT), although with a significant amount of scatter. BrGMGT abundance was not correlated to lake water pH. Seven major brGMGTs that vary in degree of methylation were identified, with *m/z* 1020, 1034 and 1048. Further, the mass chromatograms of the *m/z* 1020 and 1034 brGMGTs show an interesting distribution of peaks, which likely relates to the occurrence of distinct brGMGT isomers. This structural complexity is higher than previously observed in peats and marine sediments. Principal component analysis of the fractional abundance of bacterial tetraether lipids revealed the brGMGTs behave similarly to one another but differently from both the 5- or 6-methyl brGDGTs. This suggests the brGMGTs are produced by a common source organism and are methylated at a different position. The distribution of the seven brGMGTs showed considerable correlation with MAAT. This variability was captured in a new proxy index (the brGMGTI), which showed a strong positive linear relationship with MAAT. Lacustrine brGMGTs show potential to be applied to ancient settings to provide information about paleoclimate.

Keywords: GMGT; H-GDGT; GDGTs; Tetraethers; Lakes; Palaeotemperature; Membrane lipids; Sediments

1. INTRODUCTION

There are thousands of climate records extracted from ice sheets and deep sea sediments to elucidate Earth's dynamic climate history. Although marine and ice core records form an integral part of our knowledge, a lack of research from continental and equatorial areas causes gaps in our understanding of past climate, as climate in these areas can be markedly different than the poles or oceans

* Corresponding authors at: NIOZ Royal Netherlands Institute for Sea Research, Department of Marine Microbiology and Biogeochemistry, and Utrecht University, PO Box 59, 1790 AB Den Burg, Texel, the Netherlands.

E-mail addresses: allix.baxter@nioz.nl (A.J. Baxter), jaap.damste@nioz.nl (J.S. Sinninghe Damsté).

https://doi.org/10.1016/j.gca.2019.05.039
0016-7037/

(Otto-Bliesner et al., 2006; Blome et al., 2012; Loomis et al., 2017). Hence, there is a need for continuous paleoclimate reconstructions from continental equatorial regions. Organic biomarkers in lacustrine sedimentary records have the potential to reveal past changes in temperature, including proxies that may generate quantitative paleoclimate data (see Castaneda and Schouten, 2011 for a review). These proxies include fossilized cell membrane lipids. By modifying the structure of their membrane lipids, microbial populations adjust their membrane's permeability and fluidity to minimize the loss of energy caused by ion diffusion across the membrane (Albers et al., 2000; Weijers et al., 2007).

Glycerol dialkyl glycerol tetraethers (GDGTs) are a group of membrane spanning lipids produced by some species of archaea and bacteria, and are found in a variety of environments, including the oceans (Schouten et al., 2002), lakes (Powers et al., 2004), rivers (Zell et al., 2013; De Jonge et al., 2014b), estuaries (Sinninghe Damsté, 2016), hotsprings (Pearson et al., 2004; 2008), peats (Weijers et al., 2006a) and soils (Weijers et al., 2006b), where they may be preserved for millions of years. Since environmental factors, including temperature, influence the distribution of the particular membrane features of GDGTs (Schouten et al., 2013), GDGTs are widely used in paleoenvironmental research to investigate past climate changes. By analyzing modern sediments where the environmental conditions are relatively well constrained, proxy calibration studies have related the distribution of GDGTs to specific environmental parameters, such as temperature and pH.

To date, the main groups of GDGTs employed for paleoenvironmental reconstructions are isoprenoid GDGTs (isoGDGTs) and branched GDGTs (brGDGTs). IsoGDGTs are synthesized by different species of archaea and show a wide structural variety (see Schouten et al., 2013 for a review). Based on the stereochemistry of the glycerol moieties, brGDGTs are believed to be produced by bacteria (Weijers et al., 2006a). Acidobacteria were shown to produce a building block of brGDGTs, *iso* diabolic acid, and small amounts of brGDGTs have been detected in a few species (Sinninghe Damsté et al., 2011). However, a survey of almost all acidobacteria available in culture did not lead to the identification of new brGDGT-producing species, suggesting that multiple bacterial phyla may be responsible for brGDGT production (Chen et al., 2018; Sinninghe Damsté et al., 2018). BrGDGTs are typically much more abundant than isoGDGTs in soils and peat (Weijers et al., 2006a; 2006b), and often also in lake sediments (Blaga et al., 2009; Tierney et al., 2010; Loomis et al., 2011; 2012; 2014).

The structure of the first identified brGDGT is based on two *iso* diabolic acid skeletons ether-linked to two glycerol moieties (Sinninghe Damsté et al., 2000). In addition to this tetramethylated brGDGT, penta- or hexamethylated counterparts also occur with (an) additional methyl substituent (s) at C-5 (Sinninghe Damsté et al., 2000) and derivatives containing 1–2 cyclopentane moieties, likely formed by internal cyclization involving a mid-chain methyl group (Weijers et al., 2006a). De Jonge et al (2013) identified several additional penta- and hexamethylated brGDGTs in Siberian peat with the additional methyl groups at the C-6 position instead of the C-5 position. Subsequent improvements in chromatography (De Jonge et al., 2013; Hopmans et al., 2016) enabled analysis of these additional isomers and for better understanding of the environmental controls on the distribution of brGDGTs in natural settings (cf. Weijers et al., 2007; De Jonge et al., 2014a,b; Weber et al., 2015). It was found that the 6-methyl brGDGTs respond differently to environmental gradients than the 5-methyl brGDGTs. The degree of methylation of 5-methyl brGDGTs in soils (De Jonge et al., 2014a), peat (Naafs et al., 2018) and lake sediments (Russell et al., 2018) shows a strong correlation to MAAT. The greatest control on the fractional abundance of 6-methyl brGDGTs in soils appears to be pH, and the fractional abundances of the 6-methyl brGDGTs show a strong correlation with one another, which may suggest a common source organism (De Jonge et al., 2014a). In contrast to the isoGDGTs (Schouten et al., 2002), the cyclization of 5-methyl brGDGTs in soils (Weijers et al., 2007; De Jonge et al., 2014a) and peat (Naafs et al., 2018) does not appear to be linked with temperature but instead with pH, with a lower cyclization ratio corresponding to lower pH. This is also thought to hold for marine sediments where in-situ production in alkaline pore waters is surmised to cause the high fractional abundances of mono- and bicyclic tetra- and pentamethylated brGDGTs (Sinninghe Damsté, 2016). However, this is not evident for surface sediments of African lakes where the pH of lake water did not strongly influence brGDGT distributions (Russell et al., 2018).

Glycerol monoalkyl glycerol tetraethers (GMGTs) are a much less explored group of archaeal and bacterial lipids, although recently it was shown that they may have potential to be used as paleoclimate indicators (Naafs et al., 2018). GMGTs are also referred to as H-shaped GDGTs (H-GDGTs) because they are structurally similar to GDGTs but possess a covalent carbon–carbon bond connecting the two alkyl chains. GMGTs have been identified in sediments dating to the Jurassic Period, revealing that these compounds are preserved on geological timescales (Bauersachs and Schwark, 2016). The first isoGMGT, possessing no cyclopentane moieties (i.e. isoGMGT-0; Fig. 1) was identified in a hyperthermophilic methanogen (Morii et al., 1998). Subsequently, isoGMGTs with up to six cyclopentane moieties were identified in cultures of extremophilic Euryarchaeota and Crenarchaeota (Schouten et al., 2008a; Knappy et al., 2011) and (hydro)thermal settings (Jaeschke et al., 2012; Jia et al., 2014; Bauersachs and Schwark, 2016; Pan et al., 2016). IsoGMGTs have also been reported in low-temperature environments, such as lake and ocean sediments (Schouten et al., 2008b; Liu et al., 2012; Pan et al., 2016;), and more recently in peat (Naafs et al., 2018). In addition to the isoGMGTs, brGMGTs have been reported in marine sediments (Liu et al., 2012; Xie et al., 2014) and peat (Naafs et al., 2018). It has been suggested that the C-C bond between the alkyl chains enhances the archaeal membrane stability at higher temperatures (Morii et al., 1998; Schouten et al., 2008a).

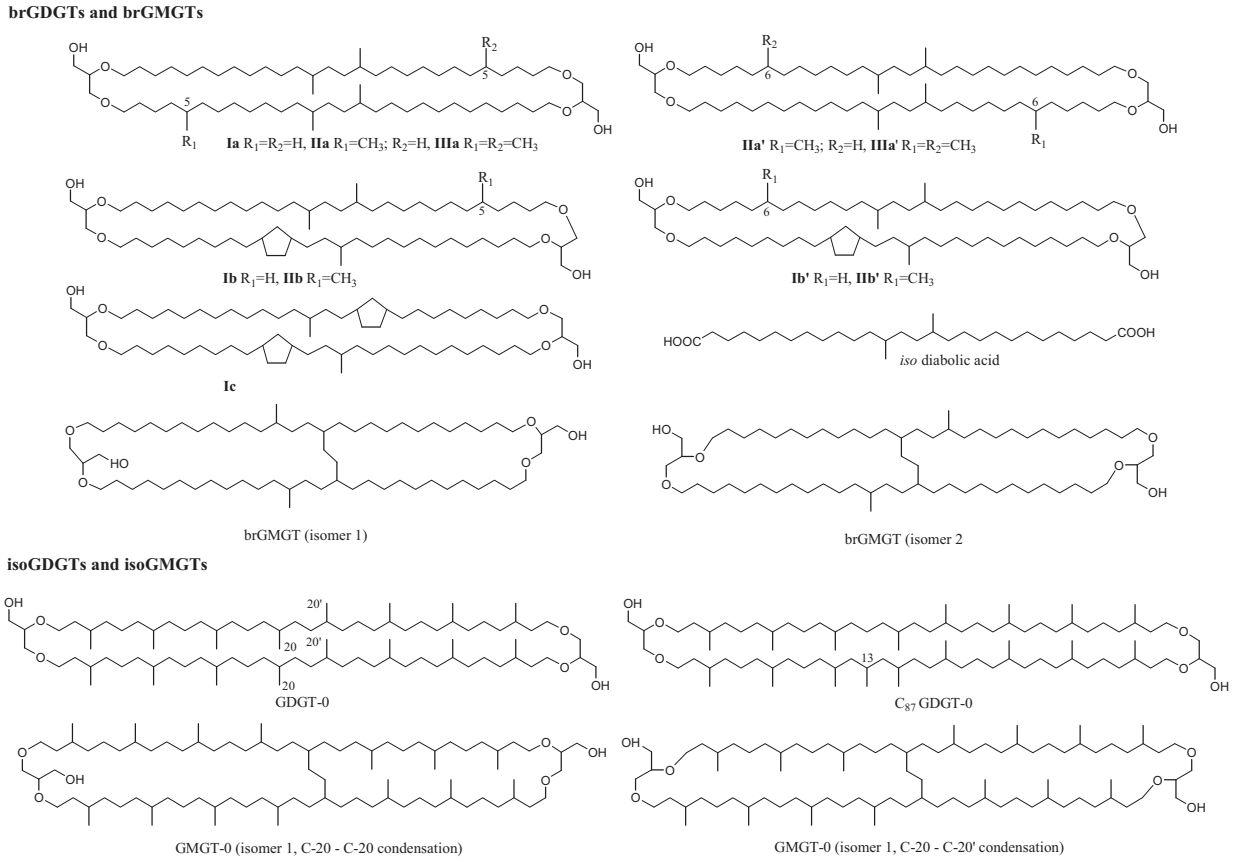

Fig. 1. Structures of isoGDGTs and brGDGTs and theoretical structures of isoGMGTs and brGMGTs.

In agreement with this, the relative abundance of isoGMGTs was found to increase with temperature across a thermal gradient in marine sediments (Sollich et al., 2017). Naafs et al. (2018) also reported a positive correlation between the relative abundance of GMGTs in a global peat data set, with the highest relative abundance of both iso- and brGMGTs occurring in tropical peatlands, although these relationships displayed significant scatter. Beyond temperature influences, there is limited evidence linking the relative abundance and distribution of isoGMGTs with varying numbers of cyclopentane rings to pH. In select terrestrial hot springs the abundance of isoGMGTs relative to isoGDGTs was found to be greater in more acidic conditions (Jia et al., 2014). To date, no evidence has been found for a connection between the occurrence of brGMGTs and pH.

African lakes have been the focus of several studies that examined the relative abundance of archaeal and bacterial tetraether lipids in sediment to calibrate and apply GDGT proxies to investigate paleoclimate (e.g. Verschuren et al., 2009; Tierney et al., 2010; Loomis et al., 2011; 2012; Sinninghe Damsté et al., 2012; Johnson et al., 2016; Russell et al., 2018). Here, we investigate the abundance and distribution of brGMGTs in 70 lake surface sediments from East Africa. This set includes lakes from a range of altitudes (615–4752 masl) and, consequently, temperatures (mean annual air temperature (MAAT) = 26.8–2.4 °C). Our data reveal the presence of a variety of brGMGTs in the lakes, and that their distribution varies with MAAT. Their potential for use in temperature reconstruction is discussed.

2. MATERIALS AND METHODS

2.1. Samples

Surface sediments of 70 lakes in tropical East Africa, mainly from Kenya, Uganda, and Ethiopia were included in this study. Fifty-nine of these are a subset of the 110 lakes previously analyzed by Loomis et al. (2011, 2012, 2014) and Russell et al. (2018). The 59 samples used for this study were selected based upon which samples contained enough material for reanalysis and sufficient concentrations of brGMGTs for integration. The surface sediments are derived from water depths from 0.3 to 180 m and are situated at a large range of altitudes, resulting in a broad range of MAAT. Complete information about the environmental setting of these samples is available in Loomis et al. (2014) and Table S1.

The dataset also includes surface sediment samples from 11 lakes in the Bale Mountains, Ethiopia (Eggermont et al., 2011), that were not included in previous GDGT calibrations. MAAT data are based on the East African lapse rate in Loomis et al. (2012) and Russell et al. (2018). Limnolog-

ical data were collected from each lake and include depth, temperature, conductivity, pH, and other measurements taken in January 2009 (dry season) and May 2010 (wet season) (Eggermont et al., 2011). Due to the shallow nature of these lakes, all values represent surface water values and data from the two months were averaged for our correlation analyses where appropriate (see Table S1).

Additionally, sediment from a core of Lake Chala (Verschuren et al., 2009) was studied. The Lake Chala sediment was sampled from core depths between 60 and 65 m and dates to the late Pleistocene (most likely within Marine Isotope Stage 5; MIS5; Moernaut et al., 2010).

2.2. Tetraether lipid analysis of the sediments

The East African lake sediments have been previously analyzed according to Hopmans et al (2016) as described by Russell et al. (2018). In this study the data set was re-examined to study the distribution of brGMGTs. The fractional abundances of the nine major brGDGTs (Ia, Ib, Ic, IIa, IIa′, IIb, IIb′, IIIa, and IIIa′; Fig. 1) and the brGMGT isomers were calculated by integration of mass chromatograms of *m/z* 1018, 1020, 1022, 1032, 1034, 1036, 1046, 1048, and 1050, assuming identical MS response factors of these tetraether lipids. Samples from the Ethiopian lakes were analyzed using the identical protocol.

The Lake Chala sediment (ca. 1 g dry weight) was extracted using a Dionex accelerated solvent extraction (ASE) system using with a 9:1 v/v mixture of dichloromethane (DCM) and methanol (MeOH). The lipid extract was dissolved in DCM/methanol (1:1, v/v), passed through a Na_2SO_4 column and dried under N_2 gas. The lipid extract was separated into apolar, ketone and polar fractions using Al_2O_3 column chromatography with eluents of hexane/DCM (9:1, v/v), hexane/DCM (1:1, v/v), and DCM/methanol (1:1, v/v) respectively, and dried under N_2 gas. The polar fraction, containing the tetraether lipids, was then re-dissolved in hexane/isopropanol (99:1, v/v) and filtered using a PTFE 0.45 μm filter. The polar fraction was analyzed by ultra-high performance liquid chromatography (UHPLC) - high resolution MS (HRMS) using an Agilent 1290 Inifinity I equipped with thermostatted auto-injector and column compartment coupled to a Q Exactive (Quadrupole Orbitrap hybrid MS) MS equipped with ion max source with APCI probe (Thermo Fisher Scientific, USA). Positive-ion APCI setting were as follows: capillary temperature 200 °C, sheath gas (N_2) 50 arbitrary units (AU); vaporizer temperature 400 °C; auxiliary gas (N_2) 5 AU, corona current 2.5 μA, APCI heater temperature 400 °C; S-lens 100 V. Chromatography was identical for UHPLC-HRMS analyses (i.e., 2 silica BEH HILIC columns in series according to Hopmans et al., 2016) as applied for the African lake surface sediment set (Russell et al., 2018). Tetraether lipids were analyzed with a mass range of *m/z* 600 to 2000 at a resolving power of 70,000 at *m/z* 200, followed by data dependent MS^2 (resolving power 17,500), in which the ten most abundant masses in the mass spectrum (with the exclusion of isotope peaks) were fragmented successively (stepped normalized collision energy 15, 20, 25; isolation window 1.0 *m/z*). An inclusion list was used with a mass tolerance of 3 ppm, comprehensively targeting ether lipids described in literature. Identification was achieved by comparison of exact mass and fragmentation spectra to literature (e.g. Knappy et al., 2009; 2015; Liu et al., 2012; Naafs et al., 2018).

2.3. Proxy calculations and statistical analysis

BrGDGT proxies were calculated using the fractional abundances of specific brGDGTs (see Fig. 1 for structures) with the following formulae:

$$MBT'_{5Me} = \frac{[Ia] + [Ib] + [Ic]}{[Ia] + [Ib] + [Ic] + [IIa] + [IIb] + [IIc] + [IIIa]} \quad (1)$$

$$DC = \frac{[Ib] + 2 * [Ic] + [IIb] + [IIb']}{[Ia] + [Ib] + [Ic] + [IIa] + [IIa'] + [IIb] + [IIb']} \quad (2)$$

The above equations capture the degree of cyclization (DC) and methylation (MBT) of branched tetraethers. These have previously been formulated by De Jonge et al. (2014a) and Sinninghe Damsté (2016) but have been simplified by elimination of certain cyclic penta- and hexamethylated brGDGTs that were below detection level or occurred in very low abundances in these samples (Russell et al., 2018).

Principal component analysis (PCA) on the correlation matrix of the fractional abundance of the of the seven brGMGTs and the nine major brGDGTs (Ia-c, IIa-b, IIa-b′, IIIa, IIIa′) was performed using the SigmaPlot 14.0 (Systat Software, Inc. 2017). All other statistical methods were as previously described (Russell et al., 2018).

3. RESULTS

Data from HPLC-MS analyses of modern surface sediments from a set of 70 East African lakes and late Pleistocene sediments from the Lake Chala core were (re-) investigated for the abundance and distribution of bacterial lipids.

3.1. Presence of brGMGTs in East African lake sediments

Upon reinvestigation of the East African lake data set, a distinct group of polar lipids with *m/z* values of 1020, 1034 and 1048, eluting ca. 20 min after the brGDGTs with one ring, were observed (Fig. 2). These components likely represent brGMGTs, previously encountered in marine sediments and peats (Liu et al., 2012; Naafs et al., 2018). The additional carbon–carbon bond which links the two alkyl chains causes brGMGTs to elute later than their brGDGT homologues. The acyclic brGDGTs Ia, IIa and IIIa are homologues of brGMGTs with *m/z* values of 1020, 1034 and 1048. Remarkably, while the mass chromatograms of the *m/z* 1020 and 1034 brGMGTs found in peat are typified by a single peak (Naafs et al., 2018), we find more complex distributions of peaks in the East African lake sediments, with up to three successive peaks (labelled H1020a-c and H1034a-c in Fig. 2). These peaks likely relate to the presence of different brGMGT isomers with *m/z* 1020 and

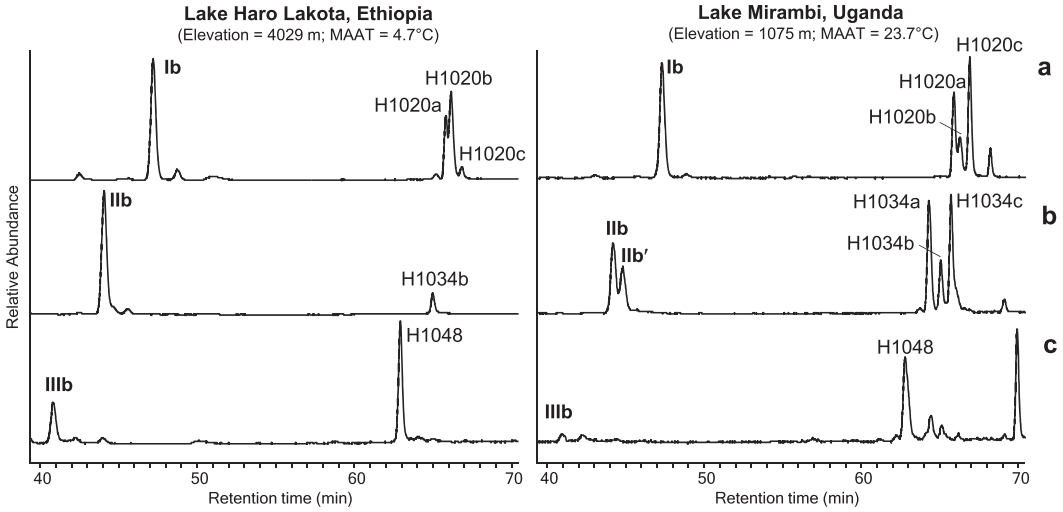

Fig. 2. Mass chromatograms for (a) *m/z* 1020, (b) *m/z* 1034, and (c) *m/z* 1048 of the polar fraction of the extracts of the surface sediments from Lake Haro Lakota, Ethiopia (elevation = 4029 m: MAAT = 4.7 °C) and Lake Mirambi, Uganda (Elevation = 1075 m: MAAT = 23.7 °C). The distributions of the brGMGTs are representative for those found in cold and warm lakes, respectively.

1034. The *m/z* 1048 mass chromatogram revealed one dominant peak but this peak was often much broader than the other peaks and its relative retention time was less constant than in case of the other isomers, both suggesting that it is comprised of (at least) two co-eluting isomers.

To confirm that these peaks indeed reflect brGMGTs, UHPLC-HRMS was performed on the polar fraction of sediments from the Lake Chala core. This sediment contained the same suite of lipids (Fig. 3a) as observed in our dataset of surface sediments. The *m/z* 1048.025 mass chromatogram revealed that the major broad peak contains a shoulder, in line with the idea that this peak is formed by at least two partially co-eluting isomers. Some minor peaks were also detected. This analysis provides evidence for the identification of all major detected compounds as brGMGT isomers. Firstly, the elemental composition of the $[M + H]^+$ ions detected fits with the elemental composition of brGMGTs (Table 1) and those of fragment ions confirm the loss of two glycerol moieties ($C_3H_6O_3$). Secondly, the MS^2 spectra of all brGMGT isomers show a distinctly different fragmentation pattern from that of the brGDGTs. Knappy et al. (2009; 2015) showed that the loss of one of the biphytanyl chains of isoGDGTs during collision induced dissociation (CID) results in product ion peaks in the so-called Region 3, while product ions of isoGMGTs only appear in Region 1 because the C—C bond connecting the two biphytanyl chains of isoGMGTs remains intact during dissociation, making the loss of a single biphytanyl chain unlikely. Product ions in Region 1 relate to the loss of small neutral molecules from the terminal glycerol moieties (Knappy et al., 2009; 2015). Similar observations have been made for the MS^2 spectra of brGMGTs (Liu et al., 2012; Naafs et al., 2018). All MS^2 spectra of the individual peaks observed in the Chala sediment show product ions consistent with their identification as brGMGTs (Fig. 4).

As observed by Naafs et al. (2018) for peats, we were also not able to detect any brGMGTs with a cyclopentane moieties as seen for brGDGTs (Weijers et al., 2006a,b); mass chromatograms of *m/z* 1018, 1032, and 1046 did not reveal any later eluting components as observed for the *m/z* 1020, 1034, and 1048 mass chromatograms (Fig. 2).

3.2. The abundance and distribution of brGMGTs in East African Lakes

Quantifiable amounts of at least some of the brGMGTs are present in all of the 70 studied lakes. Thus, acyclic brGMGTs appear commonly in East African lakes. In the *m/z* 1020, 1034 and 1048 mass chromatograms, the brGMGTs elute later than and often appear equal to or more abundant than the brGDGTs with one ring which have the same mass (Fig. 2). The %brGMGT (defined as the abundance of the seven detected brGMGTs relative to the sum of the brGMGTs and major brGDGTs) has a large range, varying from 0.5% to 31%. The highest %brGMGT was from Lake Murusi, Uganda, which has a MAAT of 22.5 °C. The lake with the lowest %brGMGT was Square Tarn, Kenya with a MAAT of 4.1 °C.

The distribution of brGMGTs shows considerable variation (Table S1). BrGMGT H1020b is on average the most abundant brGMGT in the East African lake sediment set (26.1 ± 17.8% of all brGMGTs) with H1020a (16.9 ± 6.0%), H1020c (16.2 ± 14.0%), H1048 (14.5 ± 10.2 %) and H1034b (14.4 ± 7.3%) slightly less abundant, and H1034c (7.5 ± 7.7%) and H1034a (4.3 ± 5.4%) as the least abundant brGMGTs.

To investigate potential relationships between the lipids PCA was performed on the fractional abundance of the seven brGMGTs and the nine major brGDGTs. The first three principal components (PCs) account for 75% of the total variance in this dataset (Fig. 5). What is immediately striking from the PC loading plots is that the brGMGTs, including all the different isomers, plot together in a cluster, with all brGMGTs loading positively on the PC1, PC2, and PC3 axes. Unlike the 5- (I-IIIa, I-IIb, Ic) and 6-methyl

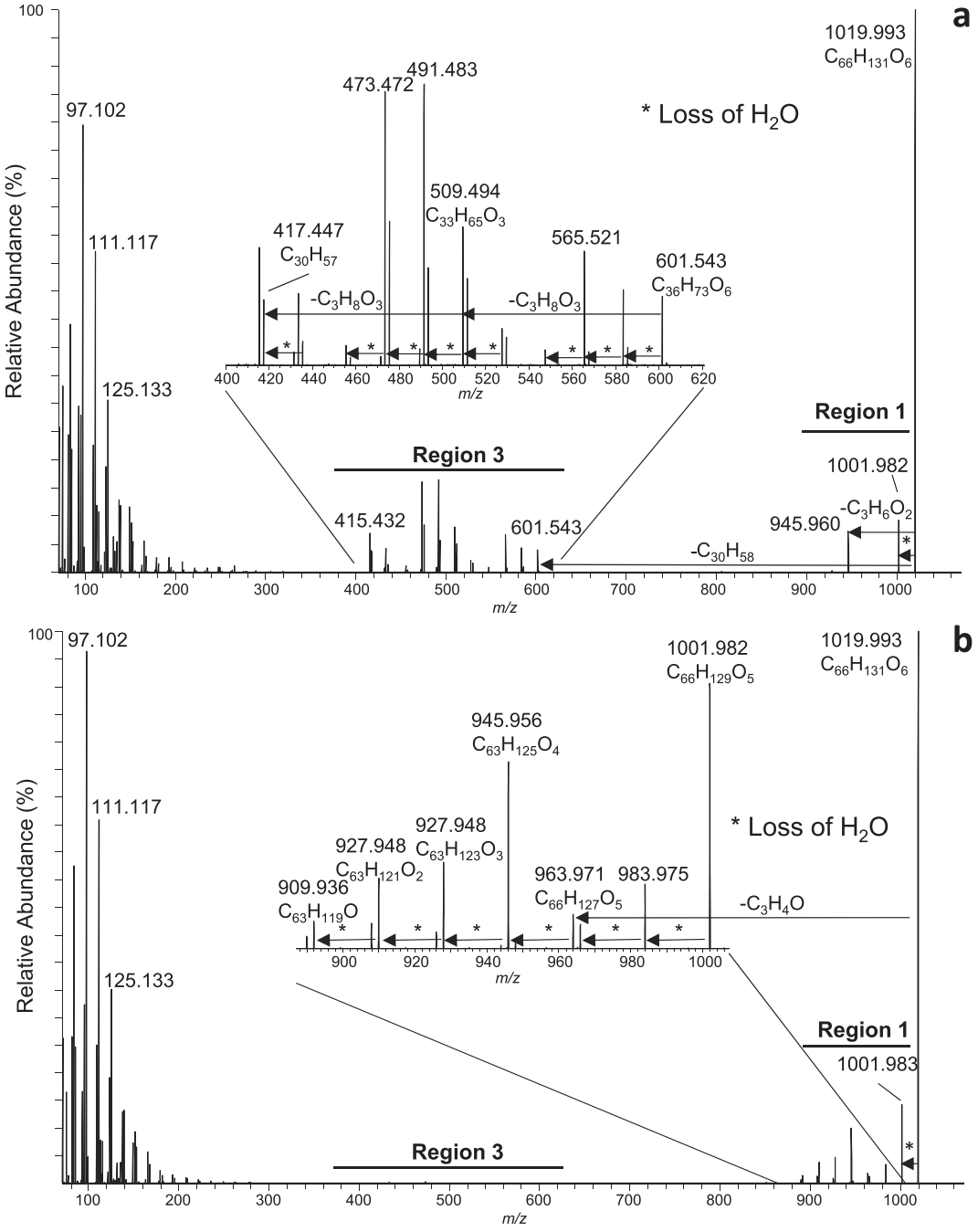

Fig. 3. MS^2 spectra showing the fragmentation patterns of (a) the regular brGDGT Ib with one ring, and (b) the brGMGT H1020c. Both branched tetraethers have a MH^+ of *m/z* 1019.994. Ib shows the presence of fragmentation ions in both region 1 and 3, whereas brGMGT H1020c only shows fragmentation occurring in region 1, which is the particular fragmentation pattern expected for GMGTs. The distinction of regions is taken from Knappy et al. (2009). Data obtained from UHPLC-HRMS analysis of the polar fraction of an extract of a sediment from Lake Chala (see also Fig. 4).

(II-IIIa′, IIb′) brGDGTs, the different isomers of the brGMGTs do not plot separately from one another. The score on PC1, which represents almost half of the variance in the dataset, primarily describes the degree of branching of the 5-methyl brGDGTs with all of the brGMGTs scoring positively together with the tetramethylated 5-methyl brGDGTs (Ia, Ib, Ic). The scores on PC1 show a significant ($r^2 = 0.88$) positive linear correlation with the degree of branching of the 5-methyl brGDGTs as expressed in the MBT'_{5Me} index. The PC2 axis separates the 5- and 6-methyl brGDGTs, with 6-methyl brGDGTs loading strongly negatively on PC2. The score on PC2 shows a significant ($r^2 = 0.72$) negative quadratic correlation with the summed fractional abundance of the 6-methyl brGDGTs.

Table 1
Elemental composition (EC) of the product ions observed in the MS^2 spectra following CID of the $[M + H]^+$ of the brGDGT Ib and the br GMGT H1020c.

$[M + H]^+$	$[F + H]^+$	EC	delta m	Number of neutral fragments lost					Previously
(*m*/*z*)	(*m*/*z*)		(mmu)	H_2O	C_3H_4O	$C_{30}H_{58}$	$C_{30}H_{58}O$	H_2	Observed[a]
brGDGT Ib									
1019.993		C66 H131 O6	−0.6	0	0	0	0	0	√
	1001.982	C66 H129 O5	−1.8	1	0	0	0	0	√
	945.959	C63 H125 O4	1.5	1	1	0	0	0	√
	601.543	C36 H73 O6	2.7	0	0	1	0	0	√
	585.548	C36 H73 O5	2.7	0	0	0	1	0	
	583.532	C36 H71 O5	2.7	1	0	1	0	0	√
	567.537	C36 H71 O4	2.7	1	0	0	1	0	
	565.521	C36 H69 O4	2.5	2	0	1	0	0	√
	547.512	C36 H67 O3	3.1	3	0	1	0	0	√
	529.505	C33H69 O4	−0.7	0	1	0	1	0	
	527.505	C33 H67 O4	1.8	1	1	1	0	0	√
	511.511	C33 H67 O3	2.9	1	1	0	1	0	
	509.494	C33 H65 O3	1.1	2	1	1	0	0	√
	493.501	C33 H65 O2	2.6	2	1	0	1	0	
	491.483	C33 H63 O2	0.4	3	1	1	0	0	√
	489.469	C33 H61 O2	2.6	3	1	1	0	1	
	475.489	C33 H63 O	1.2	3	1	0	1	0	
	473.472	C33 H61 O	0.5	4	1	1	0	0	√
	457.478	C33 H61	1.3	4	1	0	1	0	
	455.464	C33 H59	2.6	5	1	1	0	0	
	435.458	C30 H59 O	1.8	3	2	1	0	0	
	433.442	C30 H57 O	2.0	3	2	1	0	1	
	417.447	C30 H57	1.8	4	2	1	0	0	
	415.432	C30 H55	1.9	4	2	1	0	1	
brGMGT H1020c									
1019.993		C66 H131 O6	−1.1	0	0			0	√
	1001.983	C66 H129 O5	−0.1	1	0			0	√
	983.975	C66 H127 O4	2.3	2	0			0	√
	965.964	C66 H125 O3	1.4	3	0			0	√
	963.971	C63 H127 O5	3.0	0	1			0	√
	945.956	C63 H125 O4	−1.6	1	1			0	√
	927.948	C63 H123 O3	1.5	2	1			0	√
	925.938	C63 H121 O3	6.8	2	1			1	
	909.936	C63 H121 O2	−0.3	3	1			0	√
	907.921	C63 H119 O2	0.5	3	1			1	
	891.925	C63 H119 O	−0.3	4	1			0	
	889.919	C63 H117 O	0.5	4	1			1	

[a] Losses previously described for tetraether lipids by Knappy et al. (2009).

The score on PC3 separates the cyclic from the acyclic brGDGTs, with the brGMGTs grouping with the acyclic brGDGTs (I-IIIa), suggesting that the environmental controls for both the acyclic brGDGTs and brGMGTs are similar. The score on PC3 shows a significant ($r^2 = 0.53$) negative correlation with the DC index.

4. DISCUSSION

4.1. Structural considerations with respect to the brGMGTs

There is only limited information about the structure of GMGTs. IsoGMGT-0 was detected in hyperthermophilic archaea (Morii et al., 1998) but the exact position at which the two biphytanyl chains were connected remained unclear. In the archaea *Aciduliprofundum boonei* (Schouten et al., 2008a) and *Ignisphaera aggregans* (Knappy et al., 2011) isoGMGTs with 0–4 cyclopentane moieties were reported. The similar distribution of isoGDGTs and isoGMGTs suggested a direct biosynthetic link between these compound classes (Schouten et al., 2008a; Knappy et al., 2011). Lutnaes et al. (2006) elucidated the structure of a series of octaterpene tetracarboxylic acids with 4–6 cyclopentane moieties closely related to isoGMGTs in petroleum by two-dimensional NMR studies. This established the position of the bridge, i.e. between two mid-chain methyl groups of each biphytanyl chain. These tetracarboxylic acids were interpreted to be diagenetic products of isoGMGTs derived from hyperthermophilic archaea. Although direct structural identification of isoGMGTs in cultures of archaea is still lacking, the assignment of the position of the C-C bridge in their presumed diagenetic products by Lutnaes et al. (2006, 2007) is currently the best available evidence.

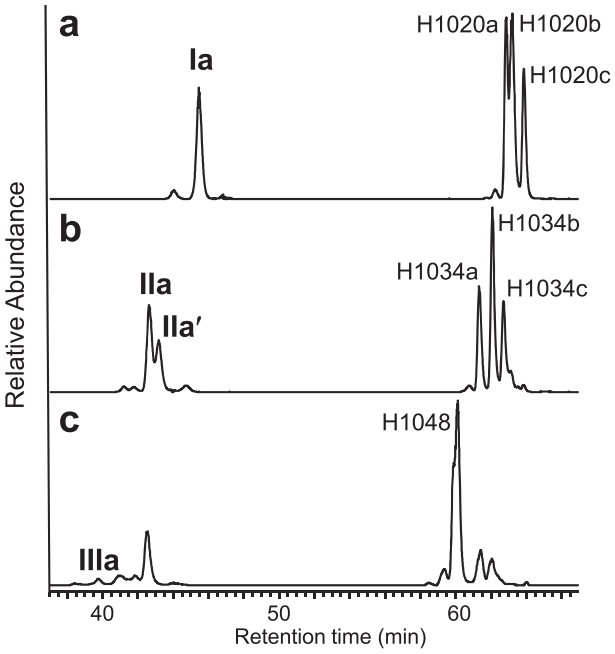

Fig. 4. Mass chromatograms (within 5 ppm mass accuracy) for (a) *m/z* 1019.994, (b) *m/z* 1034.010, and (c) *m/z* 1048.025 obtained by UHPLC-HRMS analysis of the polar fraction of an extract of a sediment from Lake Chala showing both the brGDGTs with one ring and the brGMGTs. These data reveal that the seven major brGMGT isomers detected in the surface sediments of the African lakes have the same elemental composition ($C_{66+n}H_{132+2n}O_6$, whereby n = 0–2) as those of the brGDGT with one ring.

Similarities in the presumed biosynthesis of isoGDGTs and brGDGTs have been noted (Sinninghe Damsté et al., 2011) and are based on structural similarities of the tails of the alkyl chains of the presumed building blocks, i.e. archaeol and 1,2-di-iso-pentadecyl glycerol diether. The mid-chain methyl groups of the biphytanyl chains of isoGDGTs are involved in the formation of the bridge in isoGMGTs and, hence, it seems feasible that the two alkyl groups of brGDGTs could be bridged in a similar way, i.e. by connecting two mid-chain methyl groups via a covalent bond. The enzymes responsible for the formation of isoGMGTs and brGMGTs could even be closely related, as hypothesized earlier by Naafs et al. (2018). Starting with the hypothetical 'parent' brGDGT Ia, this would result in two potential C66 brGMGT isomers (i.e. the two isomers of brGMGT in Fig. 1). The same process is theoretically possible for GDGT-0 (Fig. 1) but only one GMGT-0 peak has been reported in cultures of archaea and environmental samples (e.g. Knappy et al., 2011, Liu et al., 2012; Bauersachs and Schwark, 2016). This may be due to the co-elution of isomers with identical polarity under the HPLC conditions used in these studies.

Intriguingly, we detected three C_{66} brGMGT isomers in the African lake sediments. Liu et al. (2012) and Naafs et al. (2018) both report a single peak for the C_{66} brGMGT, even though the LC/MS method used by Naafs et al. (2018) was identical to the method used here. Clearly, further structural identification of these isomers is required, but this is hampered by the fact that ether cleavage reactions result in the formation of hydrocarbons that, in the case of GMGTs, have a molecular weight too high for analysis by GC-MS. For various GDGTs this has been a successful approach in partially resolving exact structures (Schouten et al., 1998, 2000; Sinninghe Damsté et al., 2000; Liu et al., 2012, 2016; De Jonge et al., 2014a; Knappy et al., 2015).

It is possible that the appearance of additional peaks (beyond the two peaks which may be explained by the different bridge formations) could relate to different positioning of the remaining methyl groups. In view of the known structural variation of brGDGTs, the C_{67} (H1034) and C_{68} brGMGTs (H1048) would most logically be C_{66} brGMGTs with one or two additional methyl groups. Although penta- and hexamethylated brGDGTs with methylation at C-5 or C-6 are commonly the most abundant homologues in soil, peat, and lake and marine sediments (e.g. De Jonge et al., 2014a; Sinninghe Damsté, 2016; Naafs et al., 2017; Russell et al., 2018), at present we can only speculate about the precise position of methyl groups in the brGMGTs. In fact, there is some evidence suggesting brGMGTs are not methylated at C-5 or C-6. Firstly, the PCA reveals no clear correlation between the PC loadings of the brGMGTs and their brGDGT homologues; nearly all brGMGTs score positively on PC1, PC2, and PC3 (Fig. 5a-b), whereas the 5- and 6-methyl brGDGTs plot differently from one another. Secondly, and related to this, there is no correlation between the degree of methylation of brGDGTs and brGMGTs. The scores on PC1 of the PCA correlate ($r^2 = 0.88$) linearly in the degree of branching of the 5-methyl brGDGTs as expressed in the MBT'_{5Me} index and thus predominantly responds to changes in temperature (see also Russell et al., 2018). In contrast, almost all brGMGTs load positively on PC1. Naafs et al. (2018) also detected C_{67} and C_{68} brGMGTs in peat (albeit just one isomer) and noted a clear relationship between the degree of branching of 5-methyl brGDGTs and the brGMGTs. Evidently, this relationship does not exist for lake sediments and it is therefore possible that the additional methylations may be in a different positions. Overall, this would suggest that the C_{66} - C_{68} brGMGTs are produced by a more limited group of bacteria than those that are capable of producing brGDGTs.

An observation supporting this hypothesis is that no brGMGTs containing cyclopentane rings were observed in the lake surface sediments. Naafs et al. (2018) also observed no cyclopentane-bearing brGMGTs in peats and suggested this potentially indicates that the organisms producing brGMGTs cannot biosynthesize rings, and/or that the stereochemistry of the lipid is such that the presence of the cyclopentane moiety near the middle of the alkyl chain would prevent the formation of a covalent bond between the two alkyl chains. However, considering the structure of brGDGTs this is likely not the case; even if two of the four methyl groups of the hypothetical "parent" brGDGT Ia are used to form the bridge in brGMGTs, there are still two methyl groups left for the formation of the five membered ring (see Weijers et al., 2006a; for details). Weijers et al. (2006a) established the position of

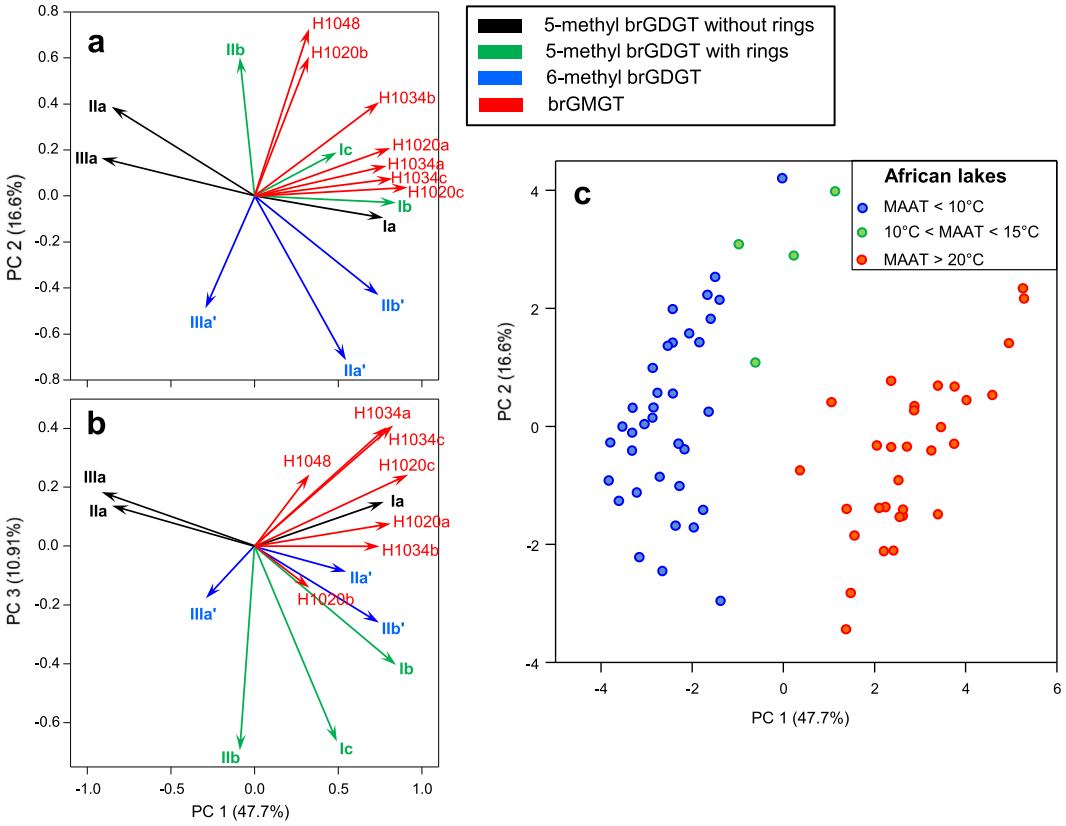

Fig. 5. PCA analysis of the fractional abundances of the major brGMGTs and brGDGTs in east African lake surface sediments. (a) and (b) Component loading plots for PC1 vs. PC2 and PC3, respectively. The color code for the different brGDGTs and brGMGTs is indicated. (c) Component score plot for PC1 and PC2 for the 70 lakes. The data points are colored according to the defined MAAT groups as indicated.

the cyclopentane moiety in brGDGTs by isolation and two-dimensional NMR but they did not establish the stereochemistry of the ring. In any case, chemically it is still possible to envisage a brGMGT with a cyclopentane moiety possessing either of the two possible stereochemistries. We therefore favor the hypothesis that the group of bacteria producing brGMGTs simply lacks the gene(s) coding for the enzyme(s) enabling this cyclization reaction. This is, for instance, the case for the Acidobacterial phylum that contains many species which biosynthesize *iso* diabolic acid, the presumed building block of brGDGTs, even with additional methyl groups at C-5 or C-6, but which does not have the biosynthetic capability to produce cyclopentane moieties (Sinninghe Damsté et al., 2018).

4.2. Environmental controls on the abundance and distribution of brGMGTs

While the %brGMGT varies widely, it is generally higher in lakes with a higher MAAT (Fig. 6a). There is, however, substantial scatter in %brGMGT for lakes with a MAAT above 20 °C, similar to the relationship between brGMGT abundances and MAAT in peat (Naafs et al., 2018; Fig. 6b). The concurrence of higher %brGMGT with higher MAAT is in line with the PCA which shows that all seven brGMGTs score positively on PC1, as PC1 is also dominated by samples with a high MBT_{5Me} index and thereby a higher temperature. This overall trend fits the idea that the connection between the two alkyl chains in GDGTs is an adaptation to increased temperature (Schouten et al., 2008a, 2013; Knappy et al., 2011). Although presently isoGMGTs have only been identified in (hyper)thermophilic and not in mesophilic archaea, it is evident from the presence of both isoGMGTs and brGMGTs in samples from non-thermophilic environments (Schouten et al., 2008b; Liu et al., 2012; Naafs et al., 2018; this study) that there must be archaea and bacteria that produce GMGTs at relatively low temperatures.

Not only does %brGMGT vary with MAAT but so also do the relative abundances and distributions of the individual brGMGTs and isomers. This is in contrast with what has been reported for the global peat data set (Naafs et al., 2018), in which there was little relationship between the relative abundances of individual brGMGTs and MAAT. This may be related to the presence of a larger number of brGMGTs isomers in the East African lake sediments. While brGMGTs H1020b, H1034b, and H1048 (probably comprised of two isomers in warm lakes) are generally present in all surface sediments of the East African lakes, isomers H1020a, H1020c, H1034a, and H1034c are more abundant in warmer lakes (e.g. Fig. 2). When the fractional abundances of these seven individual brGMGT isomers (defined as the contribution of the individual isomers to the sum of all brGMGT isomers) are plotted

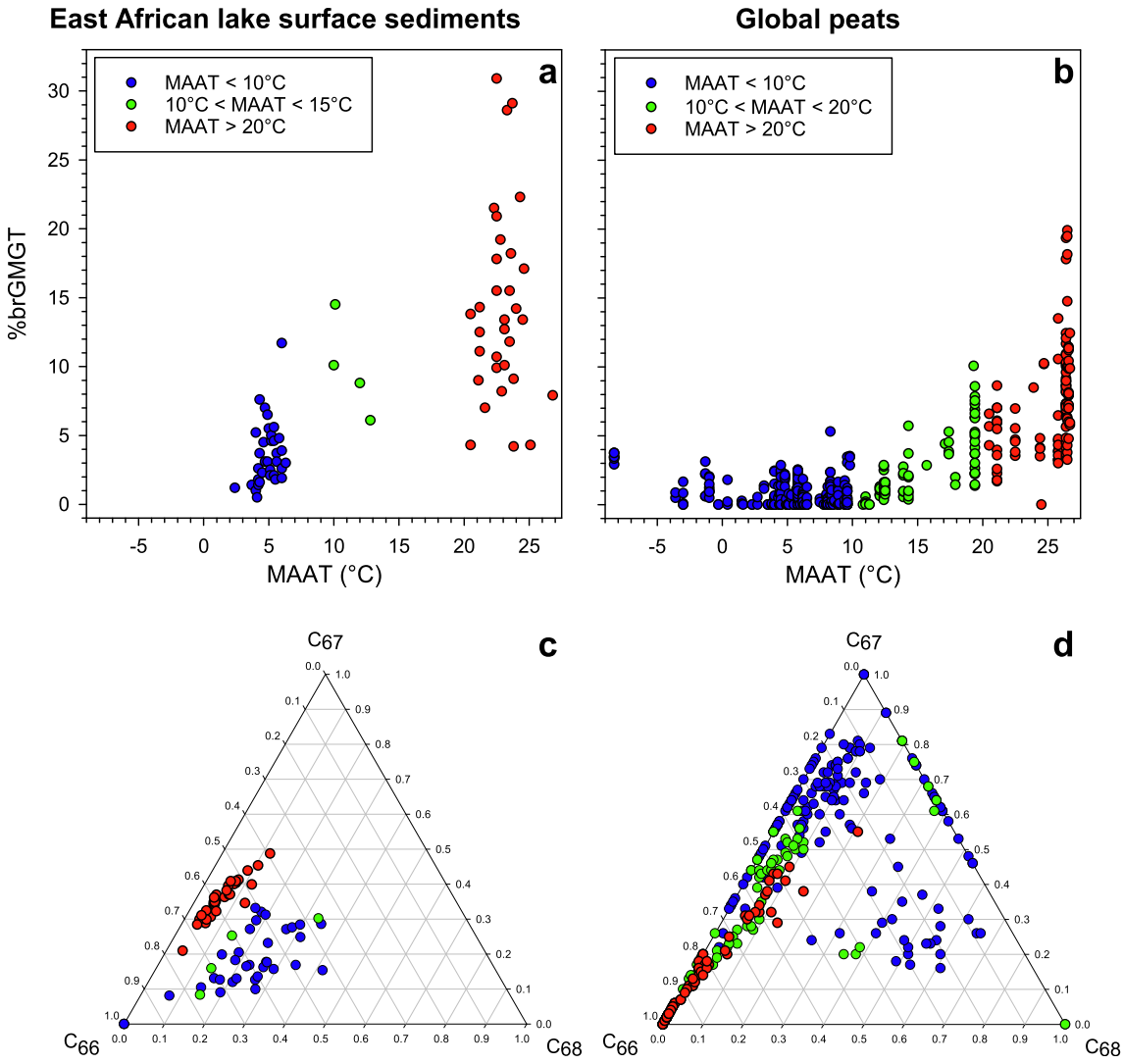

Fig. 6. The total fractional abundance of brGMGTs (%brGMGT, calculated as the relative contribution of the seven major brGMGT isomers to the sum of the nine major brGDGTs and the seven brGMGTs) versus measured MAAT for (a) the East African lake sediments and (b) the global peat set (data from Naafs et al., 2018), revealing for both datasets a general increase in %brGMGTs with increasing MAAT. The ternary diagrams show the fractional abundances of the C_{66}, C_{67}, and C_{68} brGMGTs for (c) the East African lake sediments and (d) the global peat set (data from Naafs et al., 2018). In the case of the East African lake sediments the fractional abundances of the C_{66} and C_{67} brGMGTs represent the summed fractional abundance of H1020a, H1020b, H1020c, and H1034a, H1034b, H1034c, respectively. In the case of peats, just one isomer was detected (see Naafs et al., 2018 for details). For all plots data points are colored according to the temperature ranges as indicted in the legends.

against MAAT (Fig. 7), the abundances of H1020c, H1034a, and H1034c show a positive correlation with MAAT, whereas those of H1020b and H1048 show a negative correlation with MAAT. H1020a and H1034b show no significant correlation with MAAT. This is consistent with the PCA analysis of the whole data set in which H1020b and H1048 have a lower score on PC1 and a higher score on PC2. Overall, and unlike the brGDGTs, brGMGTs with fewer methyl groups are not more abundant at higher MAAT. This would be consistent with the idea that the additional methyl groups may be at a different position. Clearly, full structural identification of these isomers (i.e. position of the bridge and additional methyl groups) is required for understanding these changes with temperature in the context of the physical properties of the membrane.

We found little evidence of linear correlations between the abundance of brGMGTs in East African lakes and lake water pH. Although the %brGMGT is slightly higher in alkaline lakes than acidic lake, the correlations of % brGMGT to pH were very weak ($r^2 = 0.14$, $n = 68$). There are also only weak linear relationships between the percentage of each brGMGT (relative to all brGMGTs) and pH, with a maximum correlation of $r^2 = 0.209$ for H1048. Furthermore, in the PCA loading plots the brGMGTs show very different loadings than the 6-methyl brGDGTs (IIa′,

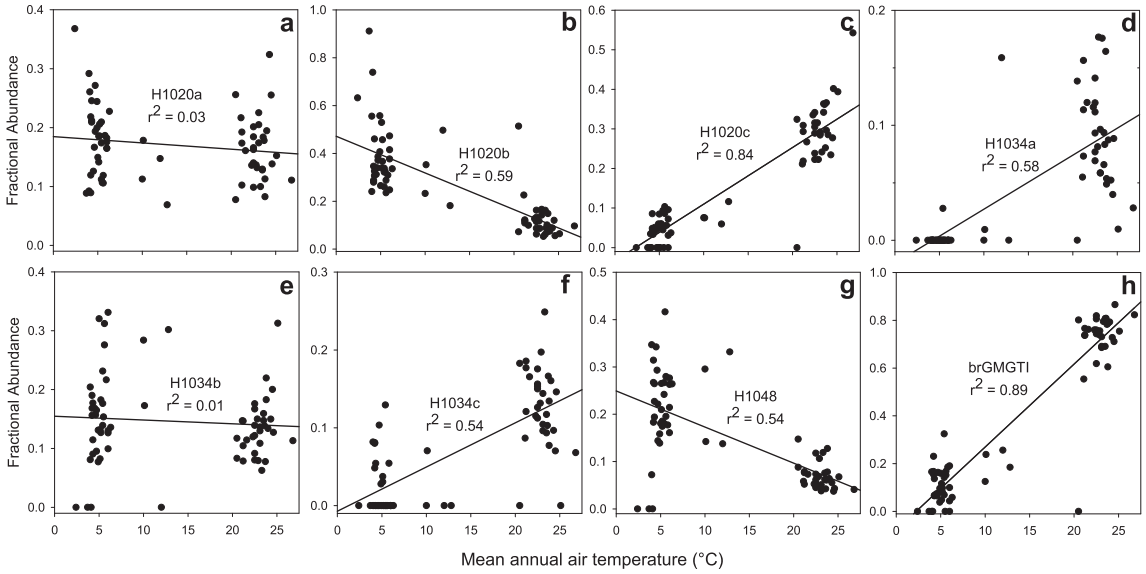

Fig. 7. The fractional abundance of each individual major brGMGT isomer (calculated as the relative contribution of the seven major brGMGT isomers to their sum) (a-g) and the brGMGTI (h) as a function of MAAT. The correlation coefficients (r^2 value) are given for each plot. Linear regression lines are shown for all correlations.

IIIa′ and IIb′) and cyclic brGDGTs (e.g. Ib, Ic, IIb), the fractional abundance of which are strongly controlled by pH in soils (De Jonge et al., 2014a). Our finding is similar to results for brGDGTs in the East African lakes, where pH shows little influence (Russell et al., 2018). However, given the uncertainty in the producer of brGMGTs and where they may reside in a lake, coupled with gradients in the pH of the lake surface, hypolimnion, and shallow sediments, it is difficult to fully test the relationship between brGMGT abundance and pH.

4.3. Potential application of brGMGTs as palaeotemperature proxies in lakes

The %brGMGT vs. MAAT relationship (Fig. 6a) is too scattered to use for reconstructing past MAAT. Naafs et al (2018) observed a similar relationship observed for peats (Fig. 6b), indicating that the %brGMGT seems to increase with increasing MAAT in both peat and lake sediment. Therefore, the %brGMGT may perhaps be used as a semi-quantitative temperature indicator in studies of ancient lake sediments in addition to other proxies.

That said, the distribution of brGMGTs is strongly controlled by MAAT in the East African lake data set (Fig. 7). Based on these relationships, a new ratio, the brGMGTs Index (brGMGTI), can be defined as shown in Eq. (3).

$$\text{brGMGTI} = \frac{[\text{H1020c}] + [\text{H1034a}] + [\text{H1034c}]}{[\text{H1020b}] + [\text{H1020c}] + [\text{H1034a}] + [\text{H1034c}] + [\text{H1048}]} \quad (3)$$

The numerator contains the relative abundance (%) of the three brGMGTs that show a positive correlation with MAAT, while the denominator contains, in addition to these three brGMGTs, two brGMGTs that show a negative correlation with MAAT (Fig. 7). The brGMGTI of the East African Lake sediments has a strong linear positive correlation to MAAT ($r^2 = 0.89$; Fig. 7h), and much less scatter at higher temperatures than the relationship of % brGMGT with MAAT. Hence this ratio can be used to predict temperature according to the model:

$$\text{MAAT} = 2.86 + 26.5 * \text{brGMGTI} \quad (4)$$

which was determined with MAAT assigned to the x-axis. In this model one outlier (Lake Mahuhura) has been excluded. The root mean square error (RMSE) of this model is 2.16 °C and r^2 is 0.94 ($p < 0.001$; Fig. 8b).

We also applied the stepwise forward selection (SFS) method (see Loomis et al., 2012; Russell et al., 2018 for details) on the relative abundances of the brGMGTs to test if this would generate an improved calibration model. This model is:

$$\text{MAAT} = 1.18 + 0.47 * [\text{H1034a}] + 0.12 * [1020\text{a}] + 0.50 * [\text{H1020c}] \quad (5)$$

This model (also with exclusion of a single outlier, Lake Mahuhura) performs almost identically to the brGMGTI model with an r^2 of 0.94 and a RMSE of 2.20 °C ($p < 0.001$; Fig. 8a).

We also tested if the addition of the set of seven brGMGTs to the suite of brGDGTs (where the abundances are normalized to the entire sum of branched tetraethers) improved upon the calibration of brGDGTs to MAAT from Russell et al. (2018) using the SFS method. However, this does not improve the model based upon brGDGTs alone (Russell et al., 2018). Interestingly, even if the brGMGTs are included the SFS selects exactly the same set of brGDGTs as in Russell et al. (2018) and does not include any of the GMGTs. It is somewhat surprising that the SFS method using the entire GDGT dataset does not include any of the brGMGTs. The main reason is likely because of the correlations of the compounds to MAAT.

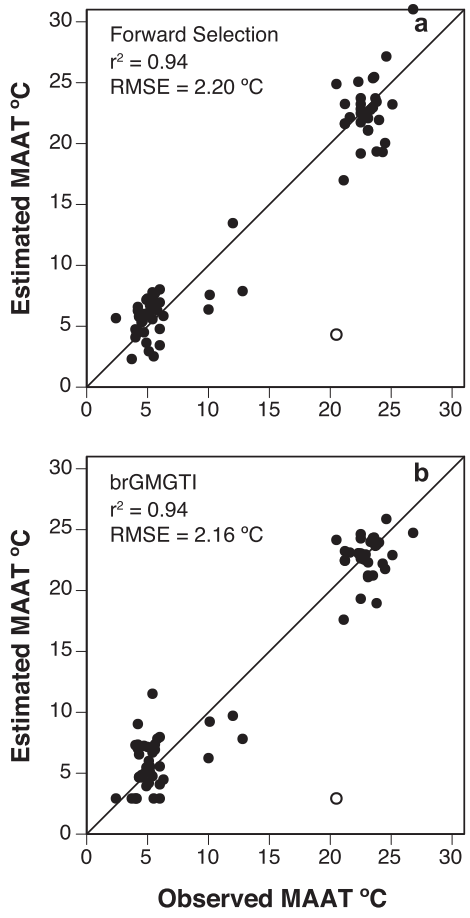

Fig. 8. New lacustrine brGMGT calibrations for mean annual air temperature based upon the brGMGTI (Eqs. (3) and (4)), and stepwise forward selection (Eq. (5)). RMSE and r^2 values are given for each calibration. In both cases one outlier was detected (Lake Mahuhura; open symbol), which was left out for calibration purposes.

Only one of the brGMGTs is correlated to MAAT with an r-value >0.8. In contrast, four brGDGTs have r-values >0.8, and the correlations are both positive and negative, so the SFS model to predict MAAT improves by including them. It is also interesting that our new brGMGT calibration models have nearly identical error statistics as the previously published models based on brGDGT fractional abundances. As noted earlier (Russell et al., 2018), this may indicate that the uncertainty in these models is strongly influenced by errors in the observed MAATs.

Although we calibrate the brGMGTs to air temperature, at present we cannot determine where in the environment brGMGTs are produced. Past studies have indicated that GMGTs are associated with anoxic settings in marine sediments (Sollich et al., 2017) and peat (Naafs et al., 2018). The lakes used in our calibration lack extensive anoxic environments in the surrounding catchment soils (many are steep, deeply weathered crater lakes) suggesting that the brGMGTs were not transported from an anoxic terrestrial source into the lakes. It seems likely that brGMGT production occurs in the lakes, potentially in their anoxic bottom waters. However, our calibration sites include several shallow lakes with fully oxygenated bottom waters, and these have a relatively high %brGMGT. This suggests that brGMGTs may also be produced by aerobic species or in the shallow anoxic sediment of the lake floor. Further investigation into the sources of brGMGTs in lake sediments is clearly needed. Nevertheless, both surface water ($r^2 = 0.97$) and bottom water ($r^2 = 0.95$) temperatures, the latter of which should also reflect the temperatures of shallow sediments, correlate strongly with MAAT in our sample set and the two rarely differ by more than ~2 °C. Therefore, it is unlikely that the location of production affects our calibrations.

The r^2 and RMSE for the brGMGTI model ($r^2 = 0.95$, RMSE = 2.0) and for the SFS model ($r^2 = 0.94$, RMSE = 2.20 °C) are both extremely strong, yet many of the samples in our dataset cluster in two distinct groups at high and low temperature. This is concerning, and reflects a lack of lakes in general at middle elevations (intermediate temperatures) in East Africa. However, the data points that do exist in our calibration with intermediate temperatures, albeit few, lie close to the linear trends in our proposed calibrations. Previous studies based on the same East African lakes have provided calibrations using bacterial lipids that have been shown to produce credible temperature reconstructions (Loomis et al., 2012; 2017). We therefore posit that the brGMGT indices and MAAT presented here can be appropriately interpreted as linearly correlated.

Based on these data it appears that brGMGTs in lake sediments have the potential to be used to predict temperature in addition to proxies based on brGDGTs. In our dataset the brGMGTI gave the best results but it should be realized that this proxy is purely an empirical one that is not based on an understanding of the underlying chemistry that influences the physical properties of the membrane. Full structural identification of these components is required to this end. Furthermore, this proxy should be tested in lake deposits (e.g. glacial-interglacial transitions, e.g. Loomis et al., 2012) before it can be applied with confidence.

5. CONCLUSION

BrGMGTs are abundant in East African lake sediment, and are likely common tetraether lipids produced in lacustrine settings. Seven major brGMGTs, which vary in the degree of methylation, were identified. This structural complexity is more than previously observed in other environments (e.g. peats and marine sediments). Assessment of the common variance of brGDGTs and brGMGTs revealed that the fractional abundances of brGMGTs predominantly co-vary with that of the brGDGT Ia but not with the 5- or 6-methyl brGDGTs, suggesting that the methyl groups may be located at a different position. The relative abundance of summed brGMGTs showed a positive correlation to MAAT but not to lake pH. The distribution of the seven brGMGT isomers showed considerable variation with MAAT. This variation was confined in the new brGMGTI, which showed a strong positive linear rela-

tionship with MAAT. Lacustrine brGMGTs show potential to be applied to ancient settings to provide information about paleoclimate but more research assessing the precise controls on the abundance and distribution of brGMGT and their exact chemical structures is required.

ACKNOWLEDGEMENTS

We thank S. Loomis for laboratory work-up of the samples, D. Dorhout for help with the UHPLC-APCI-MS analysis, H. Eggermont for collecting the surface sediments from the Ethiopian lakes, and D. Verschuren for his feedback on the manuscript. This work was supported by funding from the Netherlands Earth System Science Center (NESSC) though a gravitation grant (NWO 024.002.001) from the Dutch Ministry for Education, Culture and Science to JSSD. This work was partially also supported by a grant (NSF-EAR 1702293) from the National Science Foundation to JR. Data from this paper are available in the Pangaea database (doi:https://doi.org/10.1594/PANGAEA.901011).

APPENDIX A. SUPPLEMENTARY MATERIAL

Supplementary data to this article can be found online at https://doi.org/10.1016/j.gca.2019.05.039.

REFERENCES

Albers S. V., Van de Vossenberg J. L., Driessen A. J. and Konings W. N. (2000) Adaptations of the archaeol cell membrane to heat stress. *Front. Biosci.* **5**, 813–820.

Bauersachs T. and Schwark L. (2016) Glycerol monoalkanediol diethers: A novel series of archaeal lipids detected in hydrothermal environments. *Rapid Commun. Mass Spectrom.* **30**, 54–60.

Blaga C. I., Reichart G. J., Heiri O. and Sinninghe Damsté J. S. (2009) Tetraether membrane lipid distributions in water-column particulate matter and sediments: a study of 47 European lakes along a north–south transect. *J. Paleolimnol.* **41**, 523–540.

Blome M. W., Cohen A. S., Tyron C. A., Brooks A. J. and Russell J. (2012) The environmental contect for the origins of modern human diversity: A synthesis of regional variability in African climate 150,000–30,000 years ago. *J. Hum. Evol.* **62**, 563–592.

Castañeda I. S. and Schouten S. (2011) A review of molecular organic proxies for examining modern and ancient lacustrine environments. *Quat. Sci. Rev.* **30**, 2851–2891.

Chen Y., Zheng F., Chen S., Lui H., Phelps T. J. and Zhang C. (2018) Branched GDGT production at elevated temperature in anaerobic soil microcosm incubations. *Org Geochem.* **117**, 12–21.

De Jonge C., Hopmans E. C., Stadnitskaia A., Rijpstra W. I. C., Hofland R., Tegelaar E. and Sinninghe Damsté J. S. (2013) Identification of novel penta- and hexamethylated branched glycerol dialkyl glocerol tetraethers in peat using HPLC-MS2, GC-MS and GS-SMB-MS. *Org Geochem.* **54**, 78–82.

De Jonge C., Hopmans E. C., Zell C., Kim J., Schouten S. and Sinninghe Damsté J. S. (2014a) Occurrence and abundance of 6-methyl branched glycerol dialkyl glycerol tetraethers in soils: Implications for palaeoclimate reconstruction. *Geochim. Cosmochim. Acta* **141**, 97–112.

De Jonge C., Stadnitskaia A., Hopmans E. C., Cherkashov G., Fedotov A. and Sinninghe Damsté J. S. (2014b) In situ produced branched glycerol dialkyl glycerol tetraethers in suspended particulate matter from the Yenisei River, Eastern Siberia. *Geochim. Cosmochim. Acta* **125**, 476–491.

Eggermont H. R., Wondafrash M., van Damme K., Lens L. and Umer M. (2011) Bale Mountain lakes: Ecosystems under pressure of global change? In *Walia Special Edition on the Bale Mountains. Journal of the Ethiopian Wildlife and Natural History Society* (eds. D. Randall, S. Thirgood and A. Kinahan), pp. 171–180.

Hopmans E. C., Schouten S. and Sinninghe Damsté J. S. (2016) The effect of improved chromatography on GDGT-based palaeoproxies. *Organic Geochem.* **93**, 1–6.

Jaeschke A., Jørgensen S., Bernasconi S., Pedersen R., Thorseth I. and Früh-Green G. (2012) Microbial diversity of Loki's Castle black smokers at the Arctic Mid-Ocean Ridge. *Geobiology* **10**, 548–561.

Jia C., Zhang C. L., Xie W., Wang J. X., Li F., Wang S., Dong H., Lie W. and Boyd E. S. (2014) Differential temperature and pH controls on the abundance and composition of H-GDGTs in terrestrial hot springs. *Org Geochem.* **75**, 109–121.

Johnson T., Wern J., Brown E., Abbott A., Berke M., Steinman B. A., Halbur J., Contreras S., Grosshuesch S., Deino A. and Scholz C. (2016) A progressively wetter climate in southern East Africa over the past 1.3 million years. *Nature* **537**, 220–224.

Knappy C., Chong J. and Keely B. (2009) Rapid discrimination of archaeal tetraether lipid cores by liquid chromatography–tandem mass spectrometry. *J. Am. Soc. Mass Spectrom.* **20**, 51–59.

Knappy C. S., Nunn C. E., Morgan H. W. and Keely B. J. (2011) The major lipid cores of the archaeon *Ignisphaera aggregans*: Implications for the phylogeny and biosynthesis of glycerol monoalkyl glycerol tetraether isoprenoid lipids. *Extremophiles* **15**, 517–528.

Knappy C., Barillà D., Chong J., Hodgson D., Morgan H., Suleman M., Tan C., Yao P. and Keely B. (2015) Mono-, di- and tri-Methylated homologues of isoprenoid tetraether lipid cores in archaea and environmental samples: mass spectrometric identification and significance. *J. Mass Spectrom.* **50**, 1420–1432.

Liu X., Summons R. and Hinrichs K. (2012) Extending the known range of glycerol ether lipids in the environment: Structural assignments based on tandem mass spectral fragmentation patterns. *Rapid Commun. Mass Spectrom.* **26**, 2295–2302.

Liu X. L., De Santiago Torio A., Bosak T. and Summons R. E. (2016) Novel archaeal tetraether lipids with a cyclohexyl ring identified in Fayetteville Green Lake, NY, and other sulfidic lacustrine settings. *Rapid Commun. Mass Spectrom.* **30**, 1197–1205.

Loomis S., Russell J. and Sinninghe Damsté J. S. (2011) Distributions of branched GDGTs in soils and lake sediments from western Uganda: implications for a lacustrine paleothermometer. *Organic Geochem.* **42**, 739–751.

Loomis S. E., Russell J. M., Ladd B., Eggermont H. E., Street-Perrott F. A. and Sinninghe Damsté J. S. (2012) Calibration and application of the branched GDGT proxy on East African lake sediments. *Earth Planet. Sci. Lett.* **357–358**, 277–288.

Loomis S. E., Russell J. E., Eggermont H., Verschuren D. and Sinninghe Damsté J. S. (2014) Effects of temperature, pH, and nutrient concentrations on branched GDGT distributions in East African lakes: Implications for paleoenvironmental reconstruction. *Organic Geochem.* **66**, 25–37.

Loomis S. E., Russell J. M., Verschuren D., Morrill C., De Cort G., Damsté J. S. S., Olago D., Eggermont H., Street-Perrott F. A. and Kelly M. A. (2017) The tropical lapse rate steepened during the Last Glacial Maximum. *Sci. Adv.* **3**, e1600815.

Lutnaes B. F., Brandal Ø., Sjöblom J. and Krane J. (2006) Archaeal $_{C8}$0 isoprenoid tetraacids responsible for naphthenate

deposition in crude oil processing. *Org. Biomol. Chem.* **4**, 616–620.

Lutnaes B. F., Krane J., Smith B. E. and Rowland S. J. (2007) Structure elucidation of C_{80}, C_{81} and C_{82} isoprenoid tetraacids responsible for naphthenate deposition in crude oil production. *Org. Biomol. Chem.* **5**, 1873–1877.

Moernaut J., Verschuren D., Charlet F., Kristen I., Fagot M. and De Batist M. (2010) The seismic-stratigraphic record of lake-level fluctuations in Lake Challa: Hydrological stability and change in equatorial East Africa over the last 140 kyr. *Earth Planet. Sci. Lett.* **290**, 214–223.

Morii H., Eguchi T., Nishihara M., Kakinuma K., Konig H. and Kogaa Y. (1998) A novel ether core lipid with H-shaped C-80-isoprenoid hydrocarbon chain from the hyperthermophilic methanogen *Methanothermus fervidus*. *Bioch. Biophys. Acta - Lipids Lipid Metabol.* **1390**, 339–345.

Naafs B. D. A., Inglis G. N., Zheng Y., Amesbury M. J., Biester H., Bindler R., Blewett J., Burrows M. A., del Castillo Torres D., Chambers F. M., Cohen A. D., Evershed R. P., Feakins S. J., Gałkal M., Gallego-Sala A., Gandois L., Gray D. M., Hatcher P. G., Honorio Coronado E. N., Hughes P. D. M., Huguet A., Könönen M., Laggoun-Défarge F., Lähteenoja O., Lamentowicz M., Marchant R., McClymont E., Pontevedra-Pombal X., Ponton C., Pourmand A., Rizzuti A. M., Rochefort L., Schellekens J., De Vleeschouwer F. and Pancost R. D. (2017) Introducing global peat-specific temperature and pH calibrations based on brGDGT bacterial lipids. *Geochim. Cosmoch. Acta* **208**, 285–301.

Naafs B., McCormick D., Inglis G. and Pancost R. D.the T-GRES peat database collaborators (2018) Archaeal and bacterial H-GDGTs are abundant in peat and their relative abundance is positively correlated with temperature. *Geochim. Cosmochim. Acta* **227**, 156–170.

Otto-Bliesner B. L., Brady E. C., Clauzet G., Tomas R., Levis S. and Kothavala Z. (2006) Last glacial maximum and Holocene climate in CCSM3. *J. Clim.* **19**, 2526–2544.

Pan A., Yang Q., Zhou H., Ji F., Wang H. and Pancost R. D. (2016) A diagnostic GDGT signature for the impact of hydrothermal activity on surface deposits at the Southwest Indian Ridge. *Org Geochem.* **99**, 90–101.

Pearson A., Huang Z., Ingalls A. E., Romanek C. S., Wiegel J., Freeman K. H., Smittenberg R. H. and Zhang C. L. (2004) Nonmarine crenarchaeol in Nevada hot springs. *Appl. Environ. Microbiol.* **70**, 5229–5237.

Pearson A., Pi Y., Zhao W., Li W., Li Y., Inskeep W., Perevalova A., Romanek C., Li S. and Zhang C. L. (2008) Factors controlling the distribution of archaeal tetraethers in terrestrial hot springs. *Appl. Environ. Microbiol.* **74**, 3523–3532.

Powers L., Werne J., Johnson T., Hopmans E. C., Sinninghe Damste´ J. S. and Schouten S. (2004) Crenarchaeotal membrane lipids in lake sediments: A new paleotemperature proxy for continental paleoclimate reconstruction? *Geology* **32**, 613–616.

Russell J., Hopmans E. C., Loomis S., Liang J. and Sinninghe Damsté J. S. (2018) Distributions of 5- and 6-methyl branched glycerol dialkyl glycerol tetraethers (brGDGTs) in East African lake sediment: Effects of temperature, pH, and new lacustrine paleotemperature calibrations. *Org Geochem.* **117**, 56–69.

Schouten S., Hoefs M. J., Koopmans M. P., Bosch H.-J. and Sinninghe Damsté J. S. (1998) Structural characterization, occurrence and fate of archaeal ether-bound acyclic and cyclic biphytanes and corresponding diols in sediments. *Org Geochem.* **29**, 1305–1319.

Schouten S., Hopmans E. C., Pancost R. D. and Sinninghe Damsté J. S. (2000) Widespread occurrence of structurally diverse tetraether membrane lipids: Evidence for the ubiquitous presence of low-temperature relatives of hyperthermophiles. *Proc. Natl. Acad. Sci.* **97**, 14421–14426.

Schouten S., Hopmans E. C., Schefuß E. and Sinninghe Damsté J. S. (2002) Distributional variations in marine crenarchaeotal membrane lipids: a new tool for reconstructing ancient sea water temperatures? *Earth Planet. Sci. Lett.* **204**, 265–274.

Schouten S., Baas M., Hopmans E. C., Reysenbach A. L. and Sinninghe Damsté J. S. (2008a) Tetraether membrane lipids of *Candidatus* "Aciduliprofundum boonei", a cultivated obligate thermoacidophilic Euryarchaeote from deep-sea hydrothermal vents. *Extremophiles* **12**, 119–124.

Schouten S., Baas M., Hopmans E. C. and Sinninghe Damsté J. S. (2008b) An unusual isoprenoid tetraether lipid in marine and lacustrine sediments. *Org Geochem.* **39**, 1033–1038.

Schouten S., Hopmans E. C. and Sinninghe Damsté J. S. (2013) The organic geochemistry of glycerol dialkyl glycerol tetraether lipids: A review. *Org Geochem.* **54**, 19–61.

Sinninghe Damsté J. S., Hopmans E. C., Pancost R. D., Schouten S. and Geenevasen J. A. (2000) Newly discovered non-isoprenoid glycerol dialkyl glycerol tetraether lipids in sediments. *Chem. Commun.*, 1683–1684.

Sinninghe Damsté J. S., Rijpstra W. I. C., Hopmans E., Weijers J., Foesel B., Overmann J. and Dedysh S. (2011) 13,16-dimethyl octacosanedioic acid (iso-diabolic acid), a common membrane-spanning lipid of Acidobacteria subdivisions 1 and 3. *Appl. Environ. Microbiol.* **77**, 4147–4154.

Sinninghe Damsté J. S., Ossebaar J., Schouten S. and Verschuren D. (2012a) Distribution of tetraether lipids in the 25-ka sedimentary record of Lake Challa: Extracting reliable TEX86 and MBT/CBT palaeotemperatures from an equatorial African lake. *Quat. Sci. Rev.* **50**, 43–54.

Sinninghe Damsté J. S. (2016) Spatial heterogeneity of sources of branched tetraethers in shelf systems: The geochemistry of tetraethers in the Berau River delta (Kalimantan, Indonesia). *Geochim. Cosmochim. Acta* **186**, 13–31.

Sinninghe Damsté J. S., Rijpstra W. I. C., Foesel B. U., Huber K. J., Overmann J., Nakagawa S., Kim J. J., Dunfield P. F., Dedysh S. N. and Villanueva L. (2018) An overview of the occurrence of ether-and ester-linked iso-diabolic acid membrane lipids in microbial cultures of the Acidobacteria: Implications for brGDGT paleoproxies for temperature and pH. *Organic Geochem.* **124**, 63–76.

Sollich M., Yoshinaga M. Y., Häusler S., Price R. E., Hinrichs K. U. and Bühring S. I. (2017) Heat stress dictates microbial lipid composition along a thermal gradient in marine sediments. *Front. Microbiol.* **8**, 1550.

Tierney J. E., Russell J. M., Eggermont H., Hopmans E. C., Verschuren D. and Damsté J. S. (2010) Environmental controls on branched tetraether lipid distributions in tropical East African lake sediments. *Geochim. Cosmochim. Acta* **74**, 4902–4918.

Verschuren D., Sinninghe Damsté J. S., Moernaut J., Kristen I., Blaauw M., Fagot M., Haug G., van Geel B., De Batist M., Barker P. and Vuille M. (2009) Half-precessional dynamics of monsoon rainfall near the East African Equator. *Nature* **462**, 637–641.

Weber Y., De Jonge C., Rijpstra W. I. C., Hopmans E. C., Stadnitskaia A., Schubert C., Lehmann M., Sinninghe Damsté J. S. and Niemann H. (2015) Identification and carbon isotope composition of a novel branched GDGT isomer in lake sediments: Evidence for lacustrine branched GDGT production. *Geochim. Cosmochim. Acta* **154**, 118–129.

Weijers J., Schouten S., Hopmans E. C., Geenevasen J., David O., Coleman J., Pancost R. and Sinninghe Damsté J. S. (2006a) Membrane lipids of mesophilic anaerobic bacteria thriving in peats have typical archaeal traits. *Environ. Microbiol.* **8**, 648–657.

Weijers J., Schouten S., Spaargaren O. and Sinninghe Damsté J. S. (2006b) Occurrence and distribution of tetraether membrane lipids in soils: Implications for the use of the TEX_{86} proxy and the BIT index. *Org Geochem.* **37**, 1680–1693.

Weijers J., Schouten S., van den Donker J., Hopmans E. C. and Sinninghe Damsté J. S. (2007) Environmental controls on bacterial tetraether membrane lipid distribution in soils. *Geochim. Cosmochim. Acta* **71**, 703–713.

Xie S., Liu X. L., Schubotz F., Wakeham S. G. and Hinrichs K. U. (2014) Distribution of glycerol ether lipids in the oxygen minimum zone of the Eastern Tropical North Pacific Ocean. *Org Geochem.* **71**, 60–71.

Zell C., Kim J., Moreira-Turcq P., Abri G., Hopmans E. C., Bonnet M., Lima Sobrinho R. and Sinninghe Damsté J. S. (2013) Disentangling the origins of branched tetraether lipids and crenarchaeol in the lower Amazon River: Implications for GDGT-based proxies. *Limnol. Oceanogr.* **58**, 343–353.

Associate editor: Jochen J. Brocks